Diagn Interv Radiol 2021; 27:432–439

MUSCULOSKELETAL IMAGING
PICTORIAL ESSAY

MRI of lateral hindfoot impingement

Darshana Sanghvi

ABSTRACT
Lateral hindfoot impingement (LHI) is a subtype of ankle impingement syndrome with classic MRI findings. Biomechanically, LHI is the sequela of lateral transfer of weight bearing from the central talar dome to the lateral talus and fibula. The transfer occurs due to collapse of the medial arch of the foot, most commonly from posterior tibial tendon (PTT) and spring ligament (SL) insufficiency. Clinical features include lateral hindfoot pain, deformity, and overpronation on gait analysis. MRI changes continuously reflect the altered biomechanics as the syndrome progresses over time, including typical and often sequential changes of PTT and SL failure, increasing heel valgus, talocalcaneal and subfibular impingement, and finally lateral soft tissue entrapment. In addition to diagnosis, MRI is a useful adjunct to plan surgical treatment.

Lateral hindfoot impingement (LHI) is a subtype of ankle impingement with classic MRI findings (1). Biomechanically, LHI is the sequela of lateral transfer of weight bearing from the central talar dome to the lateral talus and fibula.

Primary LHI is rare and may occur due to an accessory anterolateral talar facet (2). Although a common accessory articulation; it can cause impingement in the occasional obese patient with subtalar eversions.

Secondary LHI is common and consequent to posterior tibial tendon (PTT) dysfunction, collapse of the medial longitudinal arch and lateral weight transfer (1). Less frequent causes of secondary LHI are neuropathic, inflammatory and degenerative arthritis of the subtalar, and transverse talar articulations. Tarsal coalitions and malunited fractures of the calcaneum are also among the uncommon causes of secondary LHI (3, 4).

MRI is useful in the diagnosis of LHI as there are several causes of lateral hindfoot pain other than impingement with overlapping clinical features. Conversely, MRI morphology and signal alteration of LHI are distinct. The multiplanar capability of MRI allows accurate assessment of the complex biomechanics and corresponding joint malalignments of LHI syndrome. Moreover, inherent sensitivity to marrow signal allows depiction of marrow edema in characteristic locations of osseous impingement. Finally, high contrast resolution permits depiction of endstage soft tissue entrapments of small ligaments and nerves (5).

In this pictorial essay, common etiologies and the resulting wide spectrum of bone and soft tissue abnormalities of LHI seen on MRI are demonstrated. The accompanying diagrams depict sequential derangements in alignment that lead to typical MRI appearances.

Biomechanics

The PTT, a powerful invertor and plantar flexor, elevates the talonavicular joint by its contraction and thus maintains the medial longitudinal arch of the foot. It stabilizes the hindfoot against valgus deformity. Hence, PTT insufficiency causes flatfoot deformity and heel valgus (6).

Most cases of LHI originate in the medial compartment from PTT dysfunction and less commonly from isolated tears of the plantar calcaneonavicular ligament (pCNL) or spring ligament (SL) (7). The PTT is the primary dynamic stabilizer of the talonavicular joint or the keystone of the foot, thus maintaining the medial arch. The SL is the primary static stabilizer. The two structures are synergists and most cases of PTT failure result in adjacent SL

From the Department of Radiology (D.S. ✉ *sanghvidarshana@gmail.com*, Kokilaben Dhirubhai Ambani Hospital, Maharashtra, India.

Received 22 April 2020; revision requested 22 May 2020; last revision received 10 August 2020; accepted 15 August 2020.

Published online 20 April 2021.

DOI 10.5152/dir.2021.20268

You may cite this article as: Sanghvi D. MRI of lateral hindfoot impingement. Diagn Interv Radiol 2021; 27:432–439

degeneration. PTT failure leads to repetitive talar head descent, thereby straining and injuring the overloaded SL. Thus, PTT failure leads to a cascade of peritalar subluxation, talar head descent, flatfoot, lateral weight transfer, heel valgus, and finally LHI (8).

Disproportionate lateral eversion from PTT failure causes abutment of the lateral process of the talus and the calcaneum at the angle of Gissane, referred to as talocalcaneal impingement (TCI). Left uncorrected, continuous eversion forces further cause the calcaneum to abut the distal fibula, referred to as subfibular impingement (SFI). Subfibular impingement can rarely be seen in isolation without TCI. TCI alone or with SFI constitutes LHI. Endstage LHI leads to soft tissue changes in the lateral gutter including peroneal tendinosis and subluxation, sural nerve compression, entrapment of the calcaneofibular ligament (CFL), and lateral adventitial bursitis (9).

Clinical features

Patients of LHI syndrome present with chronic lateral hindfoot pain, instability, deformity, and gait dysfunction with overpronation. Occasionally a remote history of medial foot pain in the past is elicited. The clinical presentation of foot pain migrating from the medial to lateral compartment over several years follows the biomechanics of PTT dysfunction in the medial compartment leading to lateral weight transfer. On clinical examination, pes planus and hindfoot valgus are noted (10). The deformity is initially flexible but turns rigid and constant as the disorder evolves. Patients with long standing history of lateral hindfoot pain and deformity may have loss of sensation along the distribution of the sural nerve with a positive Tinel's sign on examination.

Main points

- Lateral hindfoot impingement is bony abutment of the talus and calcaneum (talocalcaneal impingement) and of the fibula (subfibular impingement) with entrapment of the lateral soft tissues of the hindfoot.
- It occurs due to failure of the posterior tibial tendon and spring ligament, leading to a cascade of collapse of the medial arch of the foot and consequent lateral weight transfer. Less common causes include an accessory anterolateral talar facet, arthritis of the subtalar and transverse talar articulations, tarsal coalitions and malunited fractures. Clinical manifestations are flatfoot, heel deformity, and pain.
- MRI is useful in substantiating the clinical diagnosis and to demonstrate the entire range of bone and soft tissue changes.

Differential diagnosis

Lateral hindfoot pain may have several etiologies other than talocalcaneal and subfibular impingement. Entrapment of fat and joint capsule in the sinus tarsi has similar clinical features. Sinus tarsi syndrome may also be secondary to PTT dysfunction and occasionally precedes LHI (11). Other clinical differential diagnoses include subtalar degenerative arthritis, indolent infections, occult fractures, chondromatosis, talar osteochondritis dissecans, primary sural neuropathy and isolated peroneal tendinosis. In the clinical circumstance of a wide differential diagnosis, MRI contributes to a single, comprehensive diagnosis as well as to triage of patients into conservative and surgical management options.

Imaging of LHI

Weight-bearing frontal and lateral radiographs of the ankle and foot (Fig. 1) with possible addition of hindfoot alignment views are often the first line of assessment in patients with persistent hindfoot pain (12). If the diagnosis is evident and trial of conservative management is favored, cross-sectional imaging is not obligatory. Computed tomography (CT) is useful for pre-operative planning as it displays osseous anatomy to an advantage. For the measurements of various angles, weight-bearing cone beam CT may be superior to radiographs due to lack of superimposed bones and greater reproducibility (Fig. 2) (13). Although ultrasonography (US) does not accurately depict bone alignment and articular changes, it can depict tendon abnormalities in LHI syndrome. Tenosynovitis, tendinosis and tears of the PTT are easily diagnosed with US (14). The dynamic capability of US is useful to demonstrate tendon instability. US is also employed for guiding intra-articular injections of local anesthetics for confirmation of diagnosis and for directing sural blocks. US-guided steroid injection is a palliative option for intractable pain.

MRI, with its inherent sensitivity for bone marrow edema and multiplanar capabilities is the modality of choice to narrow the differential diagnosis of lateral hindfoot pain when radiographs are equivocal and for detailed as-

Figure 1. a, b. Weight-bearing radiographs with commonly used metrics of arch integrity and foot alignment in a case of acquired pes planus (8). Talus bone–first metatarsal axis **(a)**: anteroposterior radiograph shows the long talar axis *(solid black line)* is medially oriented as compared to the long axis of the first metatarsal *(dotted black line)* representing forefoot abduction; which is a feature of adult acquired flatfoot deformity. Normally, the two axes are close to continuous when extrapolated. Talonavicular coverage angle **(a)**: anteroposterior radiograph shows increased talonavicular coverage angle of 14°; it is the angle between the margins of the articular surfaces of the talar head *(solid white line)* and the navicular bone *(dotted white line)*. It assesses lateral rotation of the navicular bone relative to the talus bone and is normally between 0°–7°. Meary angle **(b)**: lateral radiograph shows plantar subluxation of the talar head whose long axis *(solid black line)* is no longer parallel to the long axis of the metatarsal *(dotted black line)*. In normal individuals, the angle between the two axes is close to zero, as they are nearly continuous when extrapolated. Calcaneal pitch angle **(b)**: lateral radiograph shows reduced calcaneal pitch angle of 14°. Calcaneal pitch is the angle of the plantar surface of the calcaneum *(solid white line)* to the horizontal *(dotted white line)* and is normally greater than 18°. Image Courtesy: Khushboo Pilania and Bhavin Jankharia.

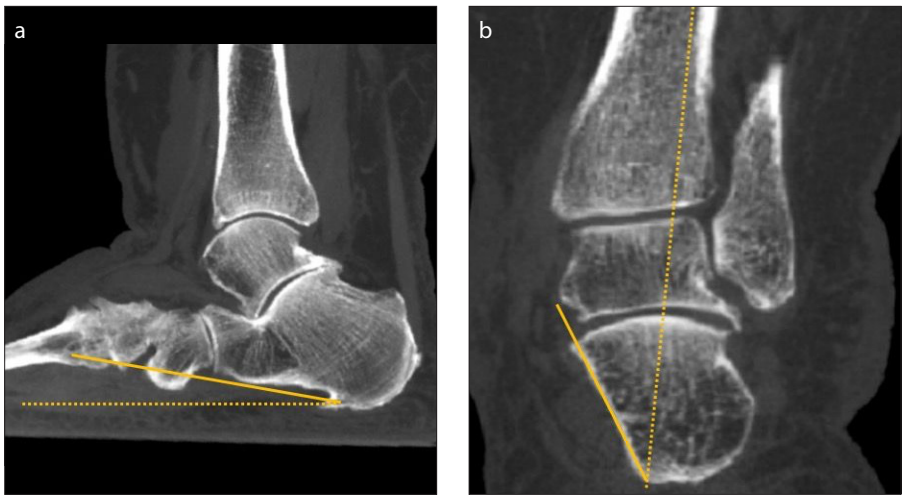

Figure 2. a, b. Weight-bearing cone beam CT showing commonly used metrics of arch integrity and foot alignment in a case of acquired pes planus (13). Sagittal reconstruction **(a)** shows reduced calcaneal pitch. Calcaneal pitch is the angle of the plantar calcaneum *(solid line)* to the horizontal *(dotted line)* and is normally more than 18°. Coronal reconstruction **(b)** shows increased heel valgus angle. Heel valgus angle is the angle of the medial margin of the calcaneum *(solid line)* to the long tibial axis *(dotted line)* and is normally less than 6°. Image Courtesy: Khushboo Pilania and Bhavin Jankharia.

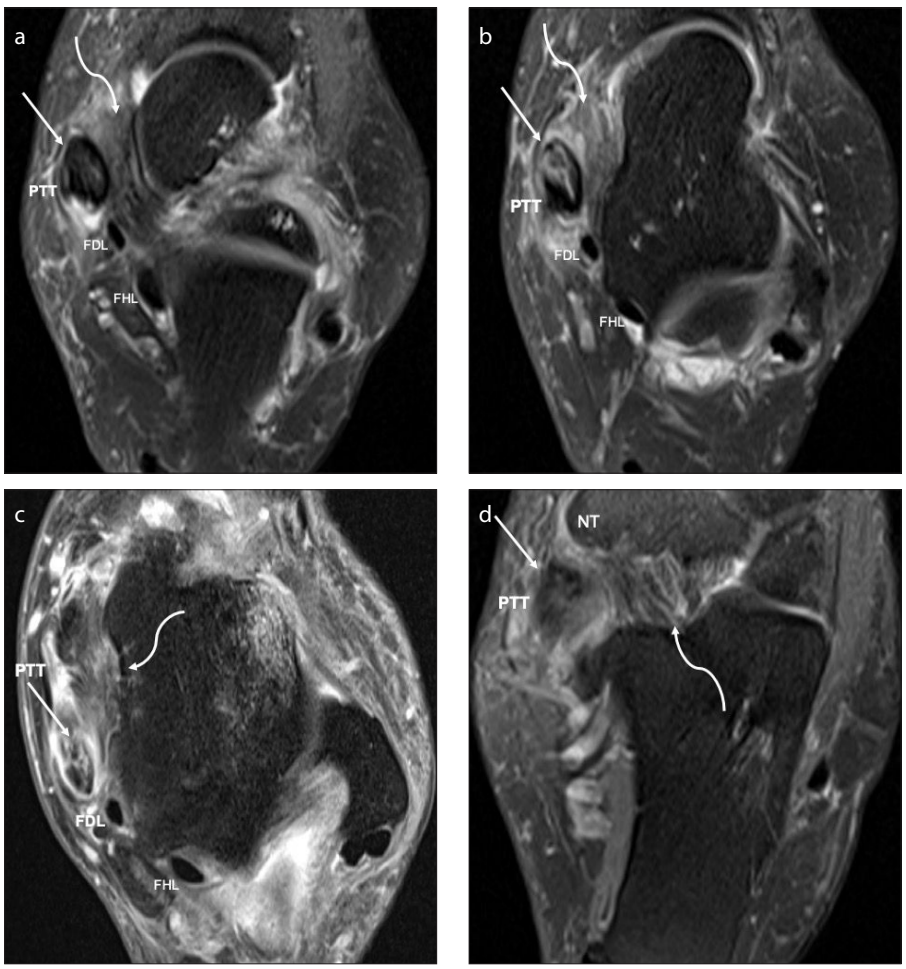

Figure 4. a–d. Grades of PTT dysfunction *(straight arrows)* with sprains of the synergistic calcaneonavicular (spring) ligament *(curved arrows)* (11, 15). Axial PD FS images in different patients. Grade 1a **(a)** is a thickened tendon without significant longitudinal splitting. Grade 1b **(b)** is a thickened tendon with significant longitudinal splits. Grade 2 **(c)** is an attenuated tendon compared to the neighboring FDL and FHL tendons. Grade 3 **(d)** is tendon rupture and avulsion from the navicular tuberosity insertion (NT). Associated degeneration and interstitial tearing of the superomedial calcaneonavicular ligament (**a–c**, *curved arrows)* and medioplantar oblique calcaneonavicular ligament (**d,** *curved arrow)* are seen.

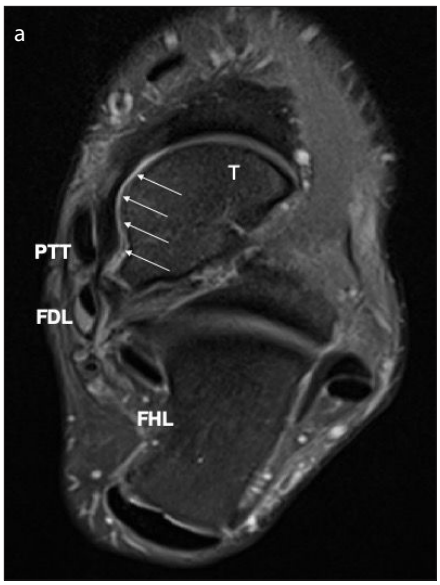

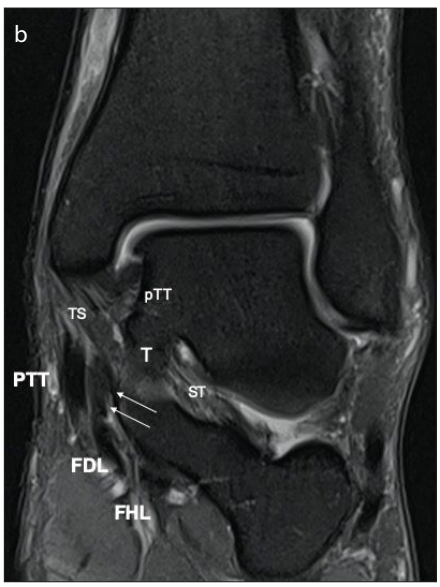

Figure 3. a, b. Normal posterior tibial tendon (PTT) and superomedial calcaneonavicular ligament (smCNL) in the posteromedial compartment of the ankle. Axial **(a)** and coronal **(b)** proton density fat suppressed (PD FS) magnetic resonance images show the PTT is anterior and medial to the flexor digitorum longus (FDL) and flexor hallucis longus (FHL) tendons. The intact smCNL *(arrows)* is in its normal location between the PTT and talus (T). After its origin from the sustentaculum tali (not shown), the smCNL passes below and medial to the talus and has a wide navicular insertion. Also seen in the coronal image **(b)** are the tibiospring ligament (TS), a component of the superficial deltoid ligament that fuses distally with the smCNL; the posterior tibiotalar ligament (pTT), the principle component of the deep deltoid ligament and ligaments of the sinus tarsi (ST).

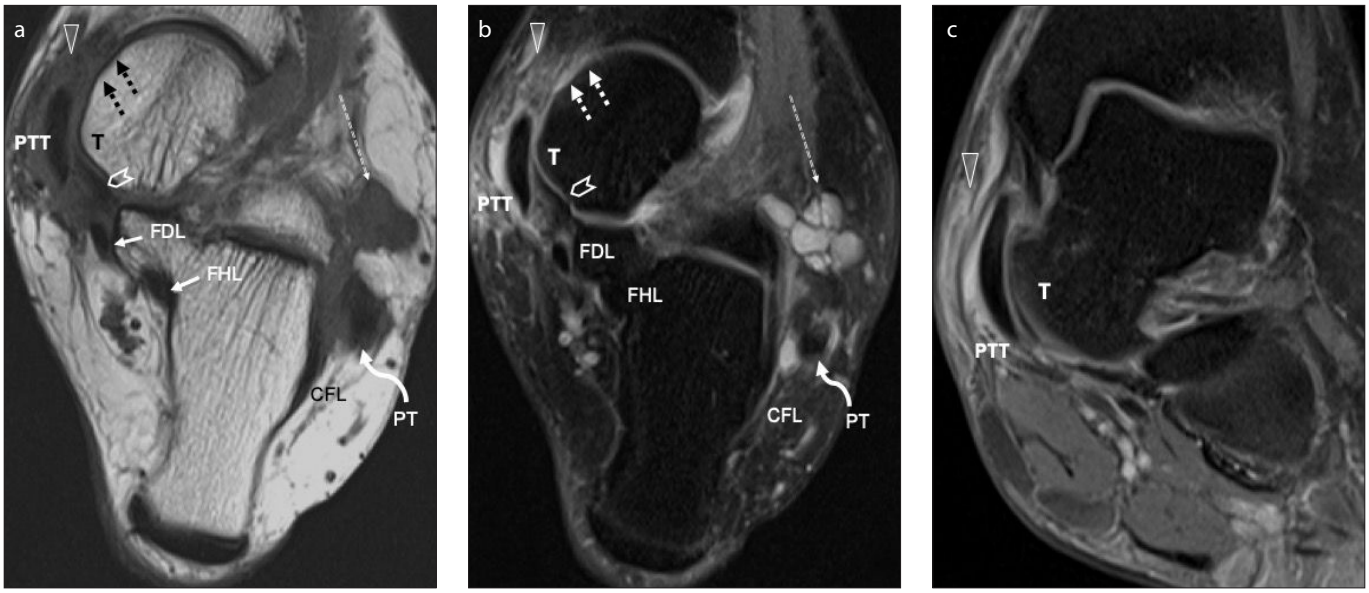

Figure 5. a–c. PTT failure without visible tear. Axial T1-weighted **(a),** axial **(b),** and coronal **(c)** PD FS magnetic resonance images show PTT tenosynovitis with adjacent subcutaneous fat stranding *(arrowhead)*. No visible tear is demonstrated in the PTT. FDL and FHL show normal morphology. The superomedial calcaneonavicular ligament (smCNL) is avulsed from its broad navicular insertion and therefore not completely visualized in its normal location between the talus (T) and the abnormal PTT, except for a proximally retracted stump (**a, b,** *chevron*). Complete CNL tear permits the PTT to abut the talus directly, without any interposing tissue of the CNL. PTT and smCNL insufficiency results in peritalar subluxation with uncovering of the medial talar head (**a, b,** *dotted arrows*). In the lateral gutter, secondary changes of subfibular impingement are seen with a multiloculated ganglion cyst (**a, b,** *dotted arrow*), entrapment of the calcaneofibular ligament (CFL) and tendinosis of the peroneal tendons (PT) (**a, b,** *curved arrows*).

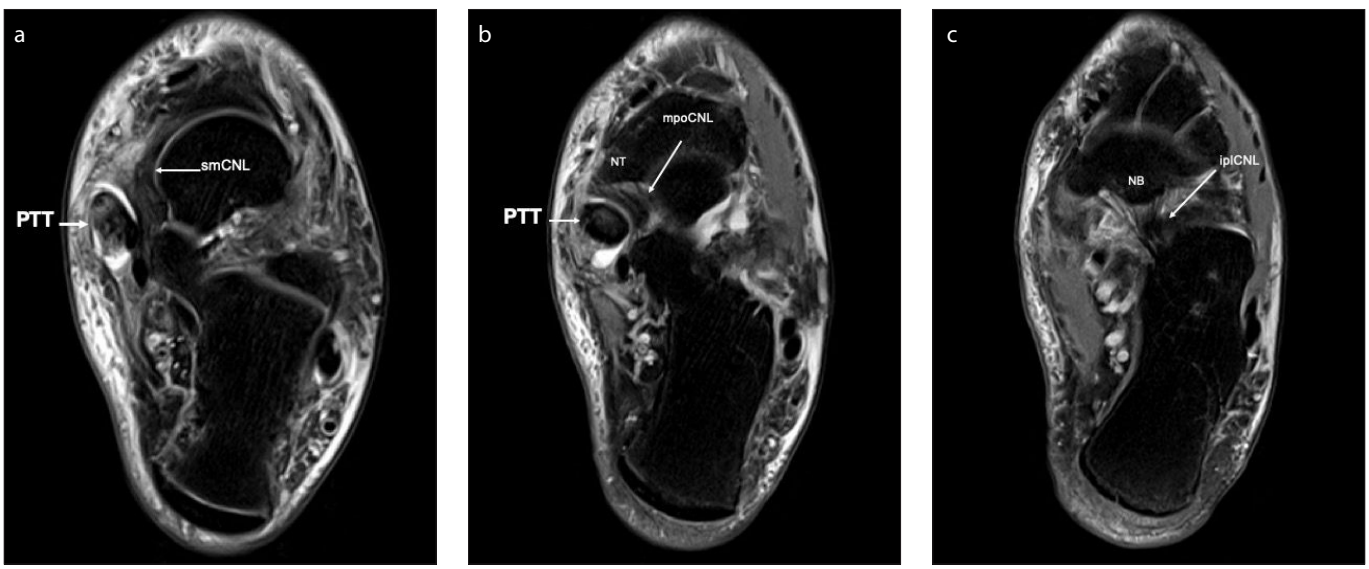

Figure 6. a–c. Degeneration of plantar calcaneonavicular ligament (pCNL) with severe PTT tendinosis. Serial axial PD FS images from cranial to caudal. The superomedial CNL (smCNL) **(a)**, the strongest and longest static stabilizer of the medial arch has a wide navicular insertion. Both the PTT and the smCNL are markedly degenerated with swelling and altered signal intensity. The medioplantar oblique CNL (mpoCNL) **(b)** and inferoplantar longitudinal CNL (ipICNL) **(c)** have a short course and narrow insertions into the navicular tuberosity (NT) and navicular beak (NB) respectively and are weaker stabilizers of the medial arch.

sessment of the entire spectrum of bone and soft tissue changes seen in LHI syndrome.

MRI features of LHI

PTT and SL anatomy

The PTT originates from the proximal tibia, fibula, and interosseous membrane and enters the foot by sharply changing angulation at the ankle in the tibial retromalleolar groove, where it is protected by the flexor retinaculum forming a fibro-osseous tunnel (6). In the midfoot and hindfoot, the PTT has a principle insertion into the navicular tuberosity and numerous and variable accessory insertions into multiple tarsal bones and metatarsal bases. It is the anterior and medial most tendon in the posteromedial compartment of the ankle and foot (Fig. 3). The flexor digitorum longus (FDL) and flexor hallucis longus (FHL) are successively located posterior and lateral to the PTT.

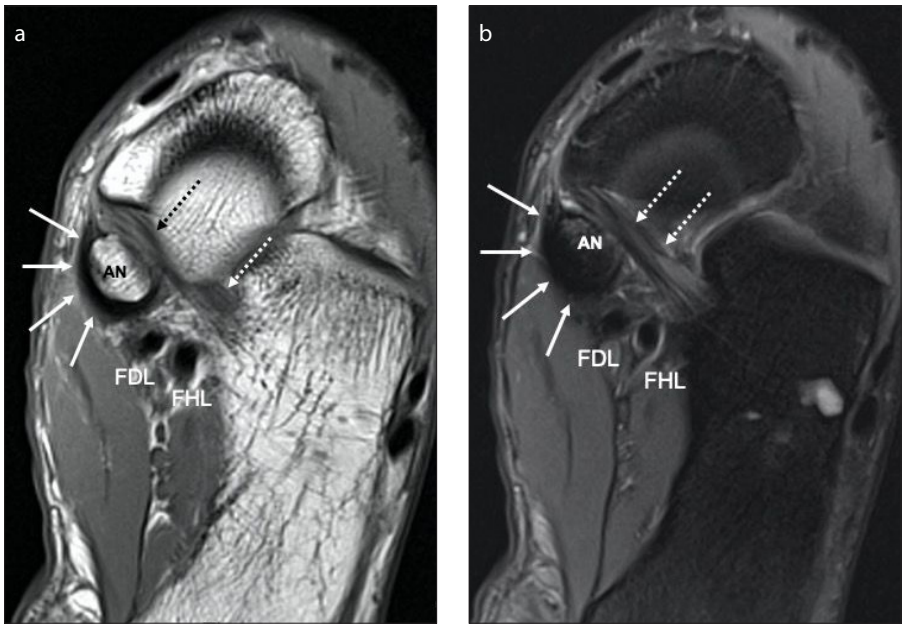

Figure 7. a, b. Symptomatic accessory navicular bone. Matched axial T1-weighted **(a)** and PD FS **(b)** images show a large type II accessory navicular (AN) bone. Note, the PTT inserts predominantly onto the ossicle rather than the more distal navicular bone, altering the angle and length of mechanical loading. Furthermore, the PTT at its insertion is stretched and wrapped around the AN *(arrows)* which will increase stress during contraction. Normal morphology of the FDL and FHL tendons permits comparison. The synergistic medioplantar oblique calcaneonavicular ligament *(dotted arrows)* is intact.

Figure 8. Heel valgus angle. Coronal T1-weighted image in a case of LHI *(arrows)* shows increased heel valgus angle (24°). It is the angle of the medial calcaneal wall as compared to the long tibial axis. Hindfoot valgus on MRI has been graded according to the angle measurements as: normal 0°–6°, mild 7°–16°, moderate 17°–26°, and severe >26° (17).

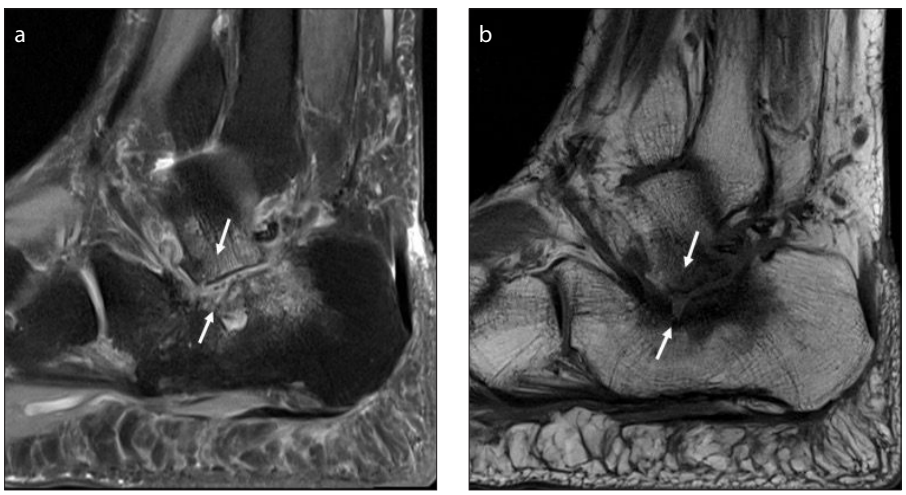

Figure 9. a, b. Talocalcaneal impingement (best demonstrated on far lateral sagittal images). PD FS **(a)** and T1-weighted **(b)** sagittal magnetic resonance images show osseous impingement of the lateral talar facet and calcaneum at the angle of Gissane *(arrows)*. PD FS images are sensitive to marrow edema and cystic change whereas T1-weighted image shows subchondral sclerosis to an advantage.

The SL, a synergist of the PTT has three main components from superomedial to inferolateral: the superomedial calcaneonavicular ligament (smCNL), the medioplantar oblique calcaneonavicular ligament (mpoCNL) and the inferoplantar longitudinal calcaneonavicular ligament (iplCNL). The smCNL (Fig. 3) creates a hammock-like structure that supports the talar head and talonavicular joint and separates the PTT from the talus bone. It is the largest and most important bundle of the pCNL and the strongest static stabilizer of the longitudinal arch. The mpoCNL and iplCFL are weak stabilizers.

PTT and SL abnormalities

PTT insufficiency as seen on MRI ranges from tenosynovitis, tendinosis and tendon elongation to frank tears, rupture, discontinuity, and tendon retraction. The prevalence of LHI significantly increases with grading of PTT tear (Fig. 4) (11, 15). However, a degenerated tendon might be elongated and dysfunctional in the absence of a visible tear (Fig. 5). The normal excursion of the PTT is merely 1-2 cm and any elongation, even by a centimeter, adversely impacts its ability to maintain the medial longitudinal arch (8). Signal alteration in the SL representing degeneration, sprains, or interstitial tearing is a sequela of PTT abnormality (Fig. 6). Although accessory navicular bones are often incidental imaging findings, type II and III variations can lead to flatfoot and pain, as the more proximal insertion of the PTT reduces the insertion angle, thereby altering biomechanics and escalating stress (Fig. 7) (16). This subset predictably presents at a younger age than PTT degeneration.

Heel valgus angle

Hindfoot valgus malalignment, the prerequisite for LHI can be objectively quantified by the hindfoot valgus angle. It is calculated as the angle between the extrapolated long tibial axis and a line along the calcaneal medial cortex on the most posterior coronal

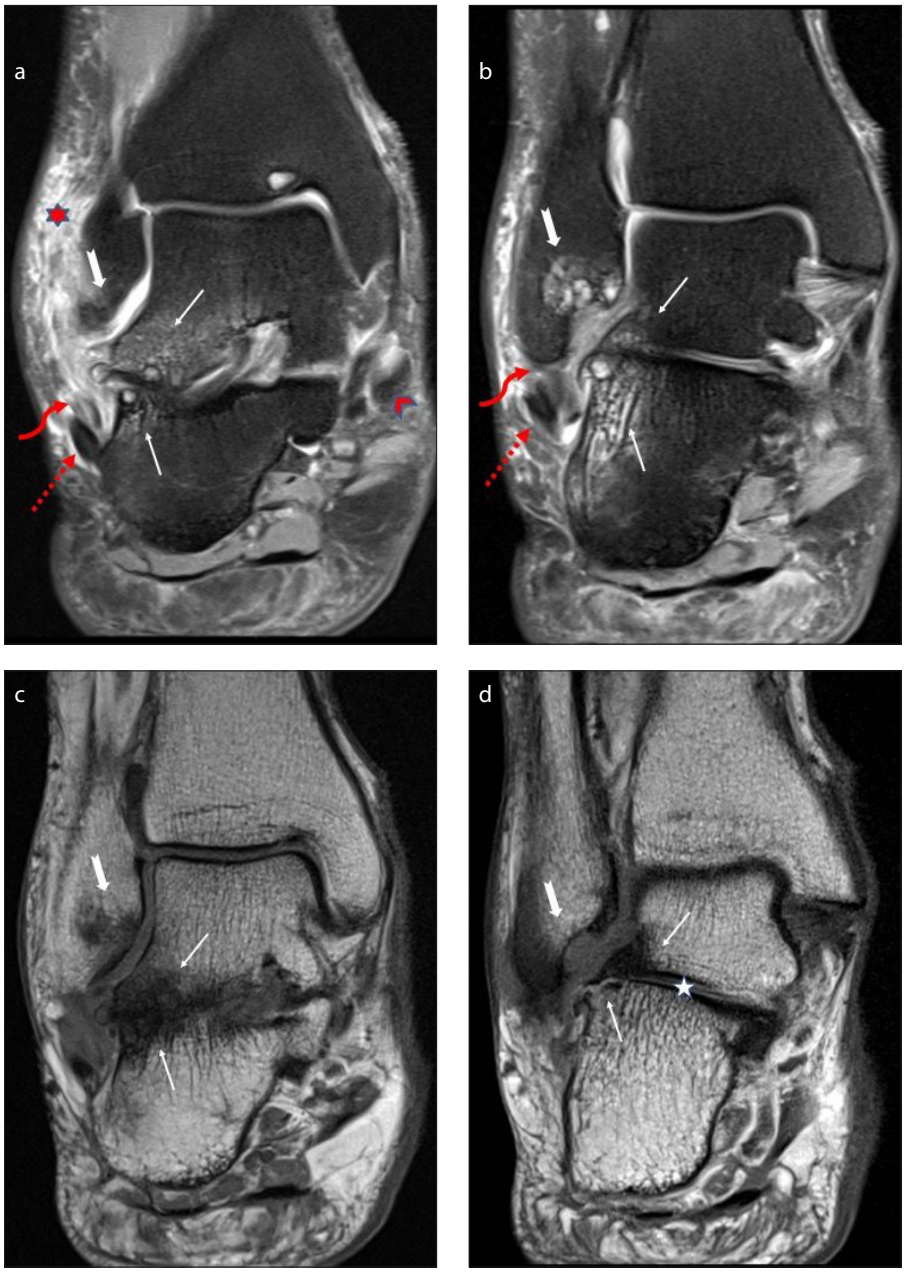

Figure 10. a–d. Combined TCI and SFI. Matched coronal PD FS **(a, b)** and T1-weighted **(c, d)** images from anterior to posterior show combined talocalcaneal impingement (TCI) *(thin white arrows)* and subfibular impingement (SFI) *(thick notched arrow)*. The sites of osseous TCI and SFI show adjoining bony spurs, subcortical marrow edema, cystic change, sclerosis and joint space loss. In the lateral gutter, PD FS images **(a, b)** show lateral adventitial bursitis (**a,** *star*), entrapment of the calcaneofibular ligament (CFL) (**a, b,** *curved arrow*) and peroneal tendinosis (**a, b,** *dotted arrow*). In the medial compartment, the PTT is focally attenuated (**a,** *arrowhead*) consistent with PTT tendinosis. Subluxation of the talocalcaneal joint (**d,** *star*) with heel valgus deformity are noted.

image that includes both the tibia and calcaneum, but excludes the sustentaculum tali (Fig. 8). The medial wall is used for the calculation as it has lesser variability due to fewer bony prominences. The normal range is less than 6 degrees (17). Most likely, this angle is underestimated on MRI as it is a non-weight-bearing technique (12).

Talocalcaneal impingement

TCI is seen as osseous abutment of the lateral facet of the talus with the calcaneum at the angle of Gissane. Subcortical sclerosis, cystic change and marrow edema are seen in the abutting talus and calcaneum (Fig. 9) with the occasional loose body. Interestingly, talar edema can be seen in asymptomatic individuals with an accessory anterolateral talar facet (18).

Subfibular impingement

SFI is seen as osseous abutment between the distal fibula and calcaneum. Occasionally, a calcaneal neofacet may form. Similar to TCI, subcortical sclerosis, cystic change and marrow edema are seen in the abutting distal fibula and calcaneum at the location of impingement (Fig. 10) (19). Marrow edema in relation to a neocalcaneal facet must be distinguished from a fibular stress fracture. In addition to marrow changes, soft tissue entrapment between the calcaneum and distal fibula appears as extensive soft tissue thickening due to fibrosis and fatty atrophy (Fig. 11).

Peroneal tendon abnormality and lateral adventitial bursitis

In the endstage of LHI, peroneal tendinosis is seen as increased signal within the enlarged longus and brevis tendons that may progress to subluxation and dislocation secondary to rupture of the peroneal retinaculum in the retromalleolar groove (Fig. 11) (9). The calcaneofibular ligament (CFL) is often trapped and thickened (Fig.12). Adventitial bursitis may be present in the lateral subcutaneous fat.

Treatment

Goals of treatment in LHI syndrome are pain relief and prevention of additional deformities. The first line of treatment is non-operative with conservative management using nonsteroidal antiinflammatory drugs, bracing, and orthotics. Activity modification and physiotherapy are advised. Image-guided injections of local anesthetics and steroids in hindfoot articulations and sural blocks help in confirmation of diagnosis for pre-operative planning. In recalcitrant cases, arthroscopic or open surgery is performed for pain alleviation and deformity management (20). Operative options include subtalar arthrodesis and calcaneal osteotomy (21). Fibular excision, peroneal tendon transposition and sural nerve neurolysis are options for subfibular impingement.

Conclusion

In conjunction with clinical examination, diagnostic and interventional radiology techniques are essential to triage patients into conservative and surgical management choices. MRI assessment further directs the orthopedic surgeon towards the appropriate operative algorithm.

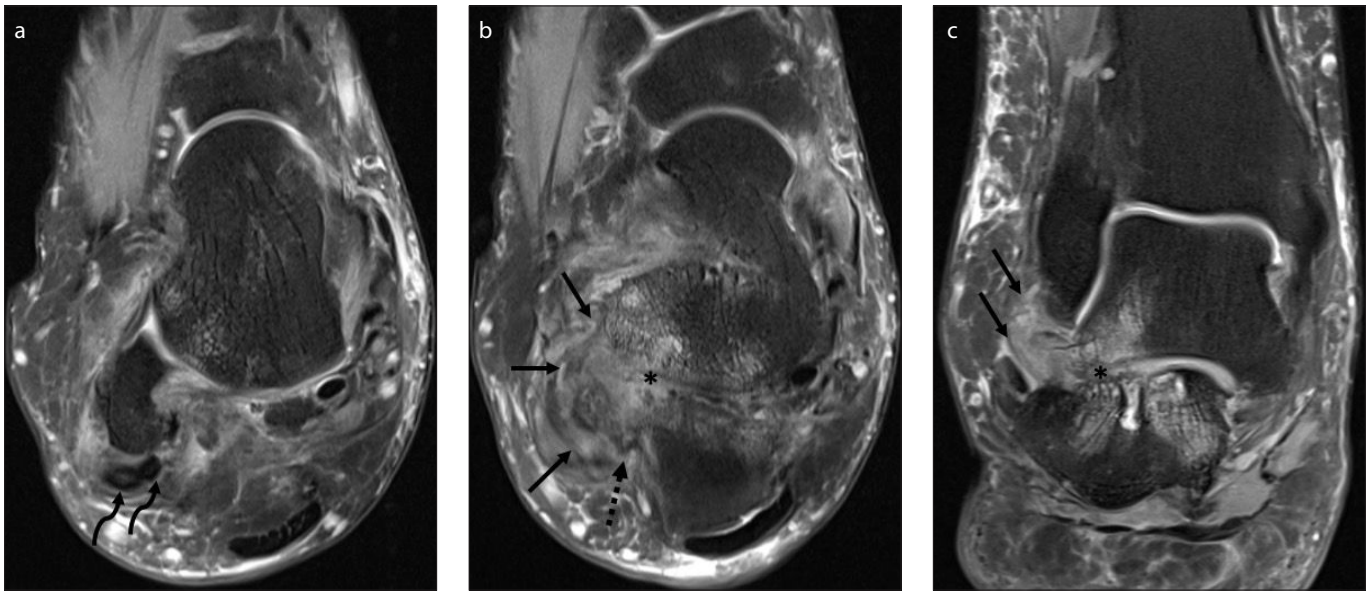

Figure 11. a–c. Soft tissue entrapment in advanced SFI. Consecutive axial PD FS images of the hindfoot at the level of **(a)** and below **(b)** the fibular tip and corresponding coronal PD FS image show mass-like soft tissue thickening (**b, c,** *arrows*) at the site of SFI with disruption of the peroneal retinaculum resulting in peroneal tendon subluxation (**a,** *curved arrows*) and chronic tear of a redundant CFL (**b,** *dotted arrow*) which is poorly identified. Also seen are changes of TCI *(asterisk)*.

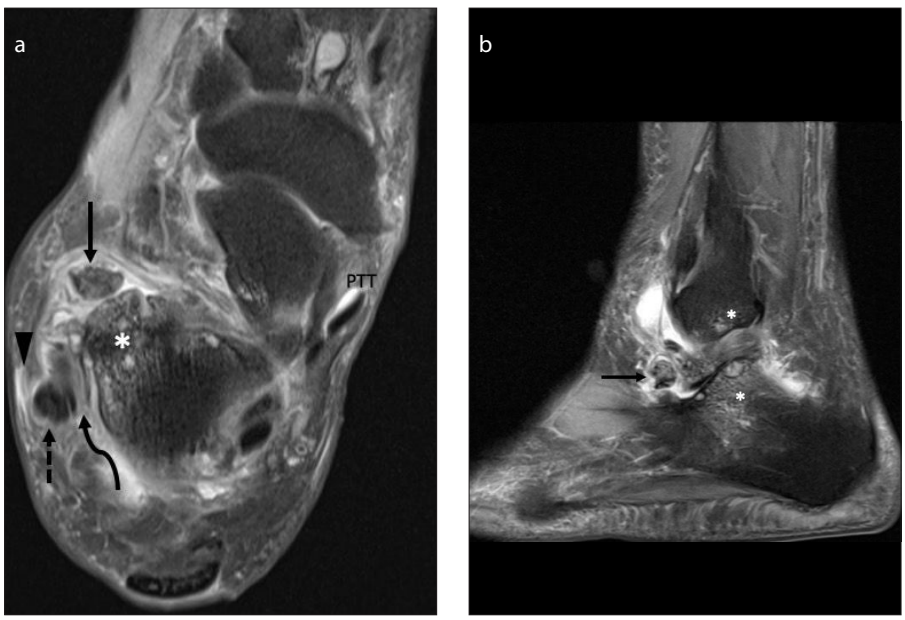

Figure 12. a, b. Loose body and lateral soft tissue entrapment in LHI syndrome. PD FS axial **(a)** and far lateral sagittal **(b)** images show a loose body *(arrow)* anterior to the talocalcaneal joint. In the subfibular space, there is peroneal tendinosis (**a,** *dotted arrow*), thickening of the trapped CFL (**a,** *curved arrow*), and mild lateral adventitial bursitis (**a,** *arrowhead*). Also seen are tenosynovitis of the PTT **(a)** and osseous impingements of LHI *(asterisks)*.

Conflict of interest disclosure

The authors declared no conflicts of interest.

References

1. Donovan A, Rosenberg ZS. MRI of ankle and lateral hindfoot impingement syndromes. AJR Am J Roentgenol 2010; 195: 595–604. [Crossref]
2. Niki H, Hirano T, Akiyama Y, Beppu M. Accessory talar facet impingement in pathologic conditions of the peritalar region in adults. Foot Ankle Int 2014; 35:1006–1014. [Crossref]
3. Zhou B, Tang K, Hardy M. Talocalcaneal coalition combined with flatfoot in children: diagnosis and treatment: a review. J Orthop Surg Res 2014; 9:129. [Crossref]
4. Reddy V, Fukuda T, Ptaszek AJ. Calcaneus malunion and nonunion. Foot Ankle Clin 2007; 12:125–135. [Crossref]
5. Persaud S, Hentges MJ, Catanzariti AR. Occurrence of lateral ankle ligament disease with stage 2 to 3 adult-acquired flatfoot deformity confirmed via magnetic resonance imaging: A Retrospective Study. J Foot Ankle Surg 2019; 58:243–247. [Crossref]
6. Ling SK, Lui TH. Posterior tibial tendon dysfunction: an overview. Open Orthop J 2017; 11:714–723. [Crossref]
7. Orr JD, Nunley JA 2nd. Isolated spring ligament failure as a cause of adult-acquired flatfoot deformity. Foot Ankle Int 2013; 34:818–823. [Crossref]
8. Flores DV, Mejía Gómez C, Fernández Hernando M, Davis MA, Pathria MN. Adult acquired flatfoot deformity: anatomy, biomechanics, staging, and imaging findings. Radiographics 2019; 39:1437–1460. [Crossref]
9. Davda K, Malhotra K, O'Donnell P, Singh D, Cullen N. Peroneal tendon disorders. EFORT Open Rev 2017; 2:281–292. [Crossref]
10. Lee MS, Vanore JV, Thomas JL, et al. Diagnosis and treatment of adult flatfoot. J Foot Ankle Surg 2005; 44:78–113. [Crossref]
11. Chhabra A, Soldatos T, Chalian M, Faridian-Aragh N, Fritz J, Fayad LM, Carrino JA, Schon L. 3-Tesla magnetic resonance imaging evaluation of posterior tibial tendon dysfunction with relevance to clinical staging. J Foot Ankle Surg 2011; 50:320–328. [Crossref]
12. Lin YC, Mhuircheartaigh JN, Lamb J, Kung JW, Yablon CM, Wu JS. Imaging of adult flatfoot: correlation of radiographic measurements with MRI. AJR Am J Roentgenol 2015; 204:354–359. [Crossref]

13. Pilania K, Jankharia B, Monoot P. Role of the weight-bearing cone-beam CT in evaluation of flatfoot deformity. Indian J Radiol Imaging 2019; 29:364–371. [Crossref]
14. Arnoldner MA, Gruber M, Syré S, et al. Imaging of posterior tibial tendon dysfunction--Comparison of high-resolution ultrasound and 3T MRI. Eur J Radiol 2015; 84:1777–1781. [Crossref]
15. Conti S, Michelson J, Jahss M. Clinical significance of magnetic resonance imaging in preoperative planning for reconstruction of posterior tibial tendon ruptures. Foot Ankle 1992; 13:208–214. [Crossref]
16. Bernaerts A, Vanhoenacker FM, Van de Perre S, De Schepper AM, Parizel PM. Accessory navicular bone: not such a normal variant. JBR-BTR 2004; 87:250–252.
17. Donovan A, Rosenberg ZS. Extraarticular lateral hindfoot impingement with posterior tibial tendon tear: MRI correlation. AJR Am J Roentgenol 2009; 193:672–678. [Crossref]
18. Aydıngöz Ü, Melih Topcuoğlu O, Görmez A, Cankurtaran T, Dilara Topcuoğlu E, Bilge Ergen F. Accessory anterolateral talar facet in populations with and without symptoms: prevalence and relevant associated ankle MRI findings. AJR Am J Roentgenol 2016; 207:846–851. [Crossref]
19. Berman Z, Tafur M, Ahmed SS, Huang BK, Chang EY. Ankle impingement syndromes: an imaging review. Br J Radiol 2017; 90: 20160735. [Crossref]
20. Seybold JD, Coetzee JC. Primary triple arthrodesis for management of rigid flatfoot deformity. JBJS Essent Surg Tech 2016; 6:e29. [Crossref]
21. Guha AR, Perera AM. Calcaneal osteotomy in the treatment of adult acquired flatfoot deformity. Foot Ankle Clin 2012; 17:247–258. [Crossref]